$Proceedings\ of\ the\ 11^{th}\ World\ Congress\ on\ Mechanical,\ Chemical,\ and\ Material\ Engineering\ (MCM'25)$

Barcelona, Spain -Paris, France - August, 2025

Paper No. HTFF 300 DOI: 10.11159/htff25.300

Prediction of Axial Wind Turbine Rotor Performances Using a Self-Corrected k-ω SST Turbulence Model

Masoud Darbandi¹, Alireza Nojavan¹, Milad Tahani¹, Gerry E. Schneider²

¹Department of Aerospace Engineering, Centre of Excellence in Aerospace Systems, Sharif University of Technology P. O. Box 11365-11155, Tehran, Iran

darbandi@sharif.edu; alireza.nojavan@ae.sharif.edu; milad.tahanipoor@ae.sharif.edu ²Department of Mechanical and Mechatronics Engineering, University of Waterloo Waterloo, Ontario, N2L 3G1, Canada gerry.schneider@uwaterloo.ca

Abstract - This study focuses on utilizing the enhanced coefficients of the k- ω SST turbulence model, derived from two-dimensional airfoil simulations, for three-dimensional rotor analysis of wind turbines. The rotor in question is part of a kilowatt-scale horizontal-axis wind turbine. This research aims to improve numerical predictions compared to experimental results. The k- ω SST model is one of the advanced turbulence models previously employed in simulations. However, the default coefficients of this model often lack sufficient accuracy in predicting aerodynamic parameters such as pressure coefficient (C_P), thrust, and torque, showing significant discrepancies with experimental data. To enhance the accuracy of these predictions, two-dimensional simulations were first conducted on the DU06-W-200 airfoil, which is used in the root section of turbine rotor. These simulations were performed across a range of Reynolds numbers and angles of attack, mirroring the turbine's operational conditions. The optimized coefficients were then applied to three-dimensional rotor analyses to replicate the turbine's real-world performance under varying operational conditions. The results demonstrate that the enhanced k- ω SST model coefficients significantly improve the prediction of C_P , thrust, and torque across different wind speeds. These findings not only reduce prediction errors but also enable more accurate aerodynamic performance analysis of wind turbine rotors. This methodology provides an effective approach to improving the accuracy of flow simulations in the design of wind turbines.

Keywords: Wind Turbine, Axial Wind Turbine, Turbulence Model, k-ω SST, CFD, Thrust, Torque, MEXICO rotor

1. Introduction

Renewable energy sources like wind are essential to the future life of human being. Horizontal-axis wind turbine (HAWT) and vertical-axis wind turbine (VAWT) play key roles in producing clean energy and reducing fossil fuel dependency. Technological advances in design and performance optimization are greatly improved their efficiency. To reduce the time and cost associated with experimental testing, numerical methods such as computational fluid dynamics (CFD) is increasingly utilized for aerodynamic evaluation. One widely used horizontal turbine is the MEXICO-rotor, which has three 4.5-meter blades designed with airfoils from the DU, RISO, and NACA families. Plaza et al [1] simulated the use of CFD and BEM methods on this rotor. At lower speeds, the BEM method performed better than the RANS method. The functions of these two methods in the field of separation in rotors at high speeds showed opposite results when compared. Furthermore, the rotor parts were analysed for their results at 35% and 92% span locations. To better understand the behavior of all three types of airfoils at different speeds and angles, it would have been beneficial to test their performance in more areas of the rotor. Darbandi et al [2] utilized the unsteady actuator line model, coupled with a three-dimensional Navier-Stokes solver and the k-ω SST turbulence model, to predict the flow field around the 5 MW NREL wind turbine. The aerodynamic forces on the rotors were calculated using the Rotor Element Momentum (BEM) theory and corrected with 3D airfoil data. Bouhelal et al [3] analysed the effects of various Reynolds-Averaged Navier-Stokes (RANS) models to assess the efficiency of horizontal-axis wind turbines under different wind conditions. Four RANS models were examined: Spalart-Allmaras, $k-\omega$ SST, $k-\epsilon$ and the transition model ($\gamma - (R_e)_{Ht}$). Regodeserves and Morros [4] used the non-linear Navier-Stokes equations (RANS) and the turbulent k-ω SST model to design stream simulations using numerical methods. The simulations were employed to represent MEXICO's complete wind turbine model, which included rotor, nozzles, and towers. The simulation of forces, torque, and pressure distribution along the rotors was relatively well-matched to the experimental results. Garcia-Ribeiro et al [5] based the simulated results of their article on three methods: k- ω SST, k- ε , Spalart-Allmaras, and $(\gamma - (R_e)_{\theta t})$ in Reynolds numbers ranging from 3×10^5 to 8×10^5 . The k- ω SST and k- ε models yielded nearly the same results. Previous models were examined both with and without zigzag strips. The k- ω SST turbulence model has been used in previous studies in a conventional manner without significant improvements. Despite simulations such as flow around wind turbine rotors, the model has not been modified perfectly. The innovation of this paper lies in enhancing the k- ω SST model by adjusting its coefficients for special fluid flow applications. The current approach is applied to simulate the three-dimensional MEXICO rotor in horizontal kilowatt-scale turbines. The modified coefficients, based on the DU airfoil family, are used for Reynolds numbers of 3×10^5 , 5×10^5 , and 7×10^5 [6], corresponding to wind speeds of 10, 15, and 24 m/s. The results include plots of torque, thrust, and improved pressure coefficients at different speeds and spanwise locations. In summary, the main contribution of this study is improving the k- ω SST model through coefficient modification, leading to increased accuracy in the analysis of the MEXICO rotor.

2. The Governing Equations

Since the flow speed around the wind turbine is much lower than the speed of sound, it can be predicted by assuming constant density, and the three-dimensional incompressible Navier-Stokes equations can be solved. For unsteady, incompressible, and three-dimensional flows, the continuity and momentum equations (using Einstein's summation convention) are written as follows [7, 8]:

$$\frac{\partial \overline{\mathbf{u}}_{\mathbf{i}}}{\partial \mathbf{x}_{\mathbf{i}}} = \mathbf{0} \tag{1}$$

$$\frac{\partial \overline{u}_{i}}{\partial t} + \overline{u_{j}} \frac{\partial \overline{u_{i}}}{\partial x_{j}} = -\frac{1}{\rho} \frac{\partial \overline{p}}{\partial x_{i}} + v \frac{\partial^{2} \overline{u_{i}}}{\partial x_{i} x_{j}} - \frac{\partial}{\partial x_{j}} (\overline{u'_{i} u'_{j}}) + S_{i}$$
 (2)

where u_i and x_i represent the components of the velocity and position vectors, respectively; t is time, ρ is density, p is pressure, and ν is the kinematic viscosity of air. As a result, the source terms S_i in the momentum equations account for the influence of the blades on the airflow. Equation (3) expresses the relationship between the relative velocity and the absolute velocity in a rotating system [3,5] as follows:

$$\mathbf{u}_{\mathbf{r}} = \mathbf{u} - \boldsymbol{\omega} \times \mathbf{r} \tag{3}$$

$$\frac{\partial \overline{u}_{i}}{\partial t} + \overline{u}_{j} \frac{\partial \overline{u}_{i}}{\partial x_{j}} + 2\omega \times u_{r} + \omega \times \omega \times r$$
(4)

where u_r is the velocity of the fluid relative to the rotating frame, u is the absolute velocity of the fluid, ω is the angular velocity vector of the rotating frame, and r is the position vector from the axis of rotation to the point of interest, which is given by [4, 8]

$$\rho \frac{\partial \mathbf{k}}{\partial t} + \frac{\partial}{\partial \mathbf{x}_{i}} (\mathbf{k} \mathbf{u}_{i}) = \frac{\partial}{\partial \mathbf{x}_{i}} \left(\Gamma_{k} \frac{\partial \mathbf{k}}{\partial \mathbf{x}_{i}} \right) + G_{k} - Y_{k}$$
 (5)

$$\rho \frac{\partial \omega}{\partial t} + \frac{\partial}{\partial x_{j}}(\omega u_{i}) = \frac{\partial}{\partial x_{j}} \left(\Gamma_{\omega} \frac{\partial \omega}{\partial x_{j}} \right) + G_{\omega} - Y_{\omega} + D_{\omega}$$
 (6)

where G_k represents the production of turbulent kinetic energy, while G_{ω} denotes the generation of the specific dissipation rate. Γ_k and Γ_{ω} are the effective diffusivities of k and ω , respectively. Y_k and Y_{ω} account for their dissipation, and D_{ω} is the cross-diffusion term [2].

3. Computational Modelling

3.1. Geometry of Wind Turbine Blade

The MEXICO wind turbine is a three-blade, upwind horizontal-axis machine with a rotor diameter of 4.5 meters. Figure 1 presents the geometry, location, and airfoil types at various sections of the MEXICO KW turbine. Figure 1 illustrates the variation of twist and chord distribution along the rotor. As shown, the rotor comprises 10 sections incorporating airfoils from the DU, NACA, and RISO families. Specifically, the DU91-W2-250 airfoil is employed from 20% to 45.6% span, the RISOE A1-21 airfoil from 54.4% to 65.6% span, and the NACA 64-418 airfoil from 74.4% span to the rotor tip. The rotors are twisted along the span, and this feature is considered in all simulations. Additionally, a constant pitch angle of -2.3° is applied to the entire rotor throughout the simulations [1,3].

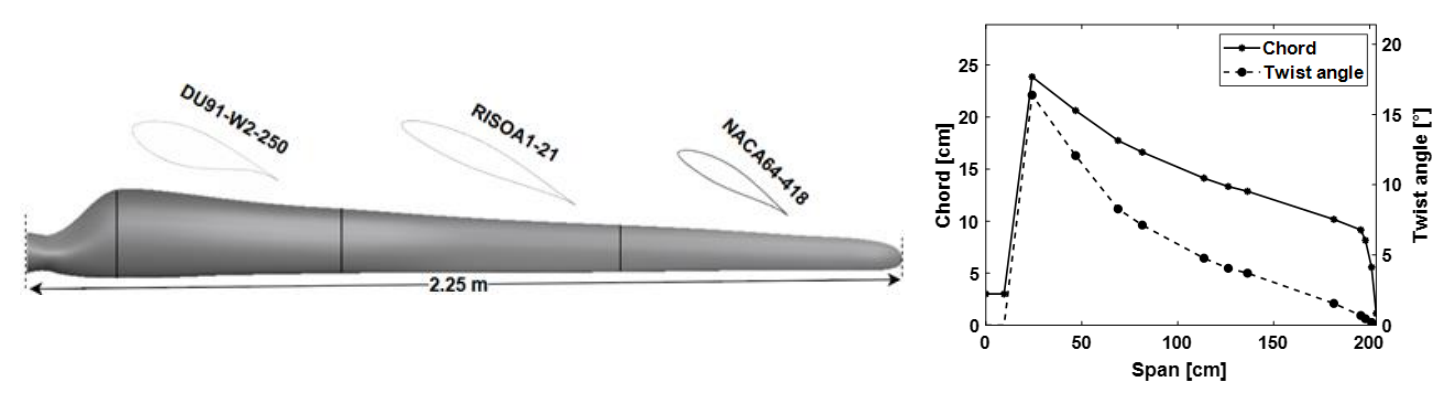


Fig. 1. Geometry of MEXICO rotor (left) and the rotor geometry and the labelling of its different rotor sections and the twist/chord distribution along the rotor span (right) [3]

3.2. Computational Domain

In this study, only a single rotor along with a portion of the hub was modelled. To reduce computational costs, one-third of the rotor was simulated, exploiting the 120° symmetry of the computational domain, representing one-third of the full rotor geometry. Previous studies [5] have also demonstrated that excluding the nacelle and tower does not significantly affect the accuracy of the results.

Regarding the computational domain dimensions, the internal rotating region has a height of 1.4 m and a radius of 2.7 m. In the external stationary domain, the distances from the plane of rotation to the inlet, outlet, and lateral boundaries are considered to be 13.5 m, 27 m, and 27 m, respectively.

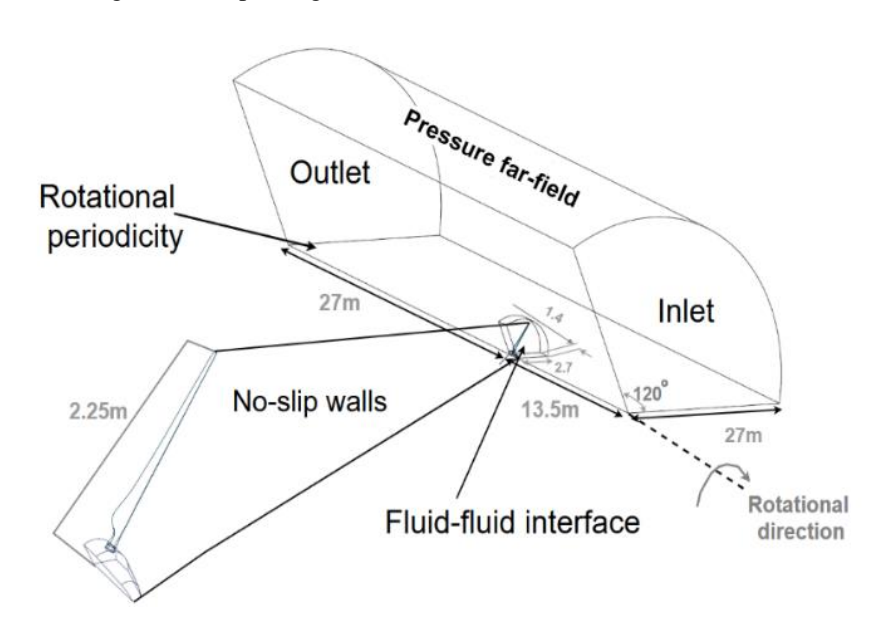


Fig 2. Sizes and boundary conditions of the domains

3.3. Mesh Generation

This study uses the boundary layer mesh. As known, the use of unstructured mesh is common for three-dimensional MEXICO rotors. A minimum boundary layer thickness of 4×10^{-4} meters was identified based on existing literature and the evaluation of typical wind turbine velocity ranges. The final mesh is an unstructured tetrahedral-prism layer mesh, used

for steady RANS simulations. Figure 3 illustrates the boundary layer formed on a cross-section of the rotor. It is worth to mention that the current work avoids using high-gradient meshes near the walls.

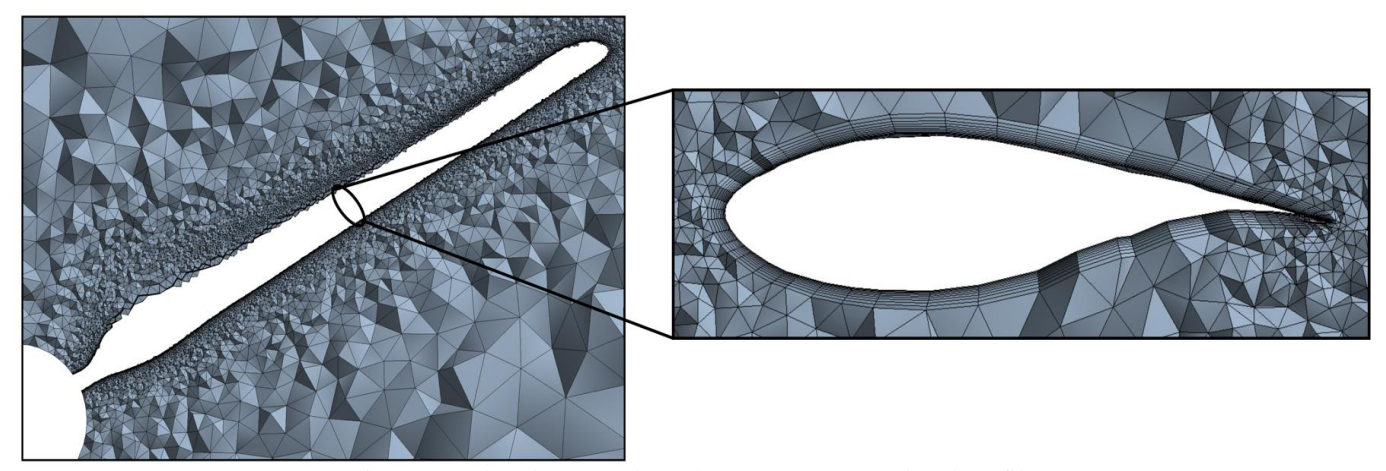


Fig 3. Boundary layer mesh on the rotor's cross-sectional profile

3.4. Boundary Conditions

Several boundary conditions were applied to the computational domains to accurately model the airflow around the rotor. At the inlet, a uniform velocity condition $U_{inlet} = U_{\infty}$ was set to represent steady incoming flow. At the outlet, a pressure boundary condition with an absolute pressure of 0 Pa was used to allow the flow to exit naturally, $P_{outlet} = 0$. To simulate the symmetry of the rotors, rotational periodicity conditions were applied to the cut side sections. Pressure farfield boundary conditions were assigned to the lateral sides, enabling pressure adjustment and flow exchange between the domain and the surrounding environment. No-slip wall conditions were applied to the rotor and hub surfaces in contact with the airflow. Figure 2 shows the locations of all these boundary conditions in the computational setup [5, 7].

3.5. Numerical Modelling

The performed CFD simulations utilize a steady-state pressure-based model and apply the SIMPLE method (Semi-Implicit Method for Pressure-Linked Equations) to solve the RANS equations. In this work, steady-state simulations are based on the numerical solution of the Navier-Stokes equations using the finite volume method along with a cell-centered discretization scheme. Spatial discretization was generally performed using second-order schemes to improve accuracy [3].

4. Discussion on the Previously Improved Coefficients of the k-ω SST Model

For the $k-\omega$ SST model, a set of fixed coefficients is considered, each of which can be optimized for different geometries to achieve improved results. These coefficients in this model are: α^* , β^* , α_{inf} , α_1 , β_1 , β_2 , $\sigma_{\omega 1,2}$, $\sigma_{k_{1,2}}$. The coefficients in the $k-\omega$ SST model each play a vital role in accurately capturing turbulence behaviour [6].

improved coefficients in each Re	3×10^{5}	5×10^{5}	7×10^{5}
α^*	1	1.2	1.2
eta_1	0.085	0.085	0.085
α_1	0.28	0.31	0.31
β*	0.09	0.09	0.09
σ_{ω_1}	2.4	2.4	2.4

Table. 2 Matrix of improved confidents for the k–ω SST model [6]

Three improved sets of coefficients were derived to improve the performance of the DU06 airfoil at Reynolds numbers of 3×10^5 , 5×10^5 and 7×10^5 , with the objective of enhancing its aerodynamic efficiency. Table 2 presents the sets of these improved coefficients [6].

A specific type of airfoil family, namely DU, is utilized in the mid-span region of the MEXICO rotor. Considering the free-stream wind speeds, this rotor section experiences Reynolds numbers approximately matching those used in the simulations of the DU airfoil. Following the past achievements, this study aims to investigate the effect of improving the coefficients of the k- ω SST turbulence model on the accuracy of the simulation results for this rotor.

5. The Result and Discussion

5.1. Mesh Independence and Validation Results

To balance solution accuracy and computational efficiency, a mesh independence study was conducted. The initial mesh consisted of 8.7 million elements, and subsequent meshes were generated by incrementally adding 2 million elements, reaching up to 19.5 million elements. Under the same conditions, with a velocity of 24 m/s, simulations were performed with different numbers of elements. Analysis of the results indicated that beyond approximately 14.1 million elements, further mesh refinement produced negligible changes in the simulation outputs. Therefore, the mesh containing 14.1 million elements was selected as optimal, providing sufficient accuracy while keeping computational costs reasonable. Figure 4 presents the results of the mesh independence study.

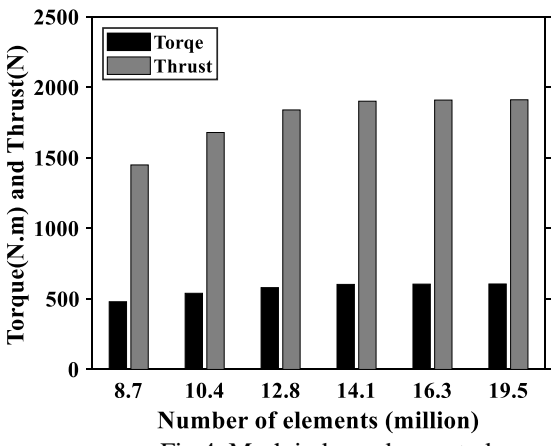


Fig 4. Mesh independence study

Therefore, the mesh containing 14.1 million elements was selected as optimal, providing sufficient accuracy while keeping computational costs reasonable. Figure 4 presents the results of the mesh independence study. The k- ω SST model simulation was initially performed using the default turbulence parameters, yielding numerical results. Figure 6 illustrates the thrust values obtained from simulations at wind speeds of 10, 15, and 24 m/s, compared against the corresponding experimental data The results were achieved with a convergence residual of 10^{-3} , typically within 500 to 1000 iterations. The comparison reveals noticeable differences between the numerical predictions and experimental measurements. Similarly, Figure 6 displays the torque results under the same flow conditions, showing comparable trends.

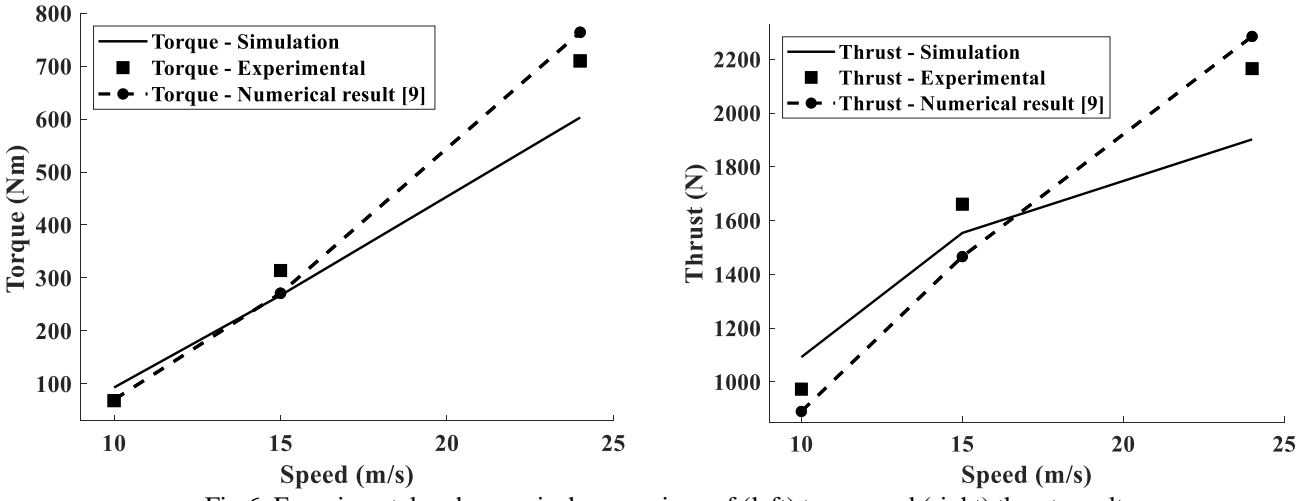


Fig 6. Experimental and numerical comparison of (left) torque and (right) thrust results

5.2. The Results

After identifying the effective coefficients from simulations using the k- ω SST model for a family of airfoils, these coefficients were categorized into two groups. The first group includes coefficients derived from simulations at a Reynolds number of 3×10^5 , whereas the second group consists of coefficients obtained at Reynolds numbers 5×10^5 and 7×10^5 , due to their high similarity. Subsequently, to evaluate these coefficients, three separate simulations were performed for each of the three specified wind speeds. The first simulation utilized the default coefficients of the k- ω SST model, the second applied the improved coefficients from the first group, and the third employed the improved coefficients from the second group.

The simulation results at a velocity of 10 m/s are presented using two sets of enhanced coefficients, as shown in Table 4. The first set of coefficients, derived at a Reynolds number of 3×10^5 , demonstrates superior performance by reducing the torque error by approximately 17.6 percent and the thrust error by 2.5 percent. The second set of coefficients also contributed marginally to improving the accuracy of the simulation results. Table 4 presents these results.

Results at a wind speed of 10 m/s	Set coefficients 1		Set coefficients 2	
	Torque	Thrust	Torque	Thrust
Experimental result	68	973	68	973
Numerical result with default coefficients	93	1092	93	1092
Numerical result with improved coefficients	81	1068	87	1052
Error for default coefficients (%)	36.7	12.2	36.7	12.2
Error for improved coefficients (%)	19.1	9.7	27.9	8.1
Percentage of improvement (%)	17.6	2.5	8.8	4.1

Table. 4 Torque and thrust values obtained using the improved coefficient set at a wind speed of 10 m/s

The simulation results at a velocity of 15 m/s indicate that the performance of both sets of coefficients is very similar. The first set, derived from a Reynolds number of 3×10^5 , and the second set, obtained from Reynolds numbers of 5×10^5 and 7×10^5 , showed nearly the same level of error reduction, with only a one to two percent difference between them. Ultimately, the second set demonstrated slightly better performance, reducing the torque error by 3.4 percent and the thrust error by 6.2 percent. Table 5 presents the obtained results.

Table. 5 Torque and thrust values obtained	using the improved	l coefficient set at a wind	speed of 15 m/s

Results at a wind speed of 15 m/s	Set coefficients 1		Set coefficients 2	
	Torque	Thrust	Torque	Thrust
Experimental result	314	1661	314	1661
Numerical result with default coefficients	267	1554	267	1554
Numerical result with improved coefficients	272	1638	278	1665
Error for default coefficients (%)	14.9	6.4	14.9	6.4
Error for improved coefficients (%)	13.3	1.4	11.5	0.2
Percentage of improvement (%)	1.6	5	3.4	6.2

The results obtained from the simulation at a wind speed of 24 m/s reveal some interesting observations. Specifically, the default coefficients outperformed those of the first set. However, this was not the case for the second set. The coefficients in the second set, derived from Reynolds numbers of 5×10^5 and 7×10^5 , were able to reduce the torque error by 10.8 percent and the thrust error by 10 percent. Table 5 shows the obtained results.

Table 6. Torque and thrust values obtained using the improved coefficient set at a wind speed of 24 m/s

Results at a wind speed of 24 m/s	Set coefficients 1		Set coefficients 2	
	Torque	Thrust	Torque	Thrust
Experimental result	710	2165	710	2165
Numerical result with default coefficients	603	1902	603	1902
Numerical result with improved coefficients	564	1887	740	2211
Error for default coefficients (%)	15	12.1	15	12.1
Error for improved coefficients (%)	20.5	12.8	4.2	2.1
Percentage of improvement (%)	-5.5	-0.7	10.8	10

Based on the obtained error percentages, the optimal set of coefficients from the two groups was selected for each wind speed. Using these selected coefficients, pressure coefficients were calculated at sections corresponding to 35%, 60%, and 82% of the span, each of which includes an airfoil from the DU, RISO, and NACA families, respectively. The results were then compared with those obtained from simulations utilizing the default coefficients. Based on the comparison of the two sets of aerodynamic coefficients at different flow velocities, the dimensionless pressure coefficient (C_p) was calculated at predefined sections. For the velocity of 10 m/s, the first set of coefficients was applied, while for velocities of 15 and 24 m/s, the second set was utilized due to its better performance at higher Reynolds numbers. Figures 7, 8, and 9 illustrate the C_p distributions at wind speeds of 10, 15, and 24 m/s, respectively.

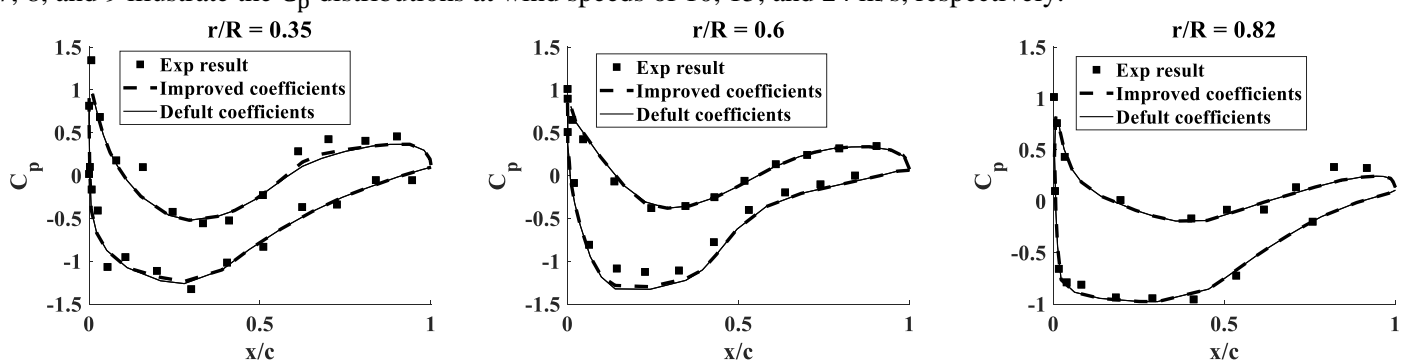


Fig 7. Pressure coefficient distributions at tree spanwise sections for wind velocity = 10 m/s

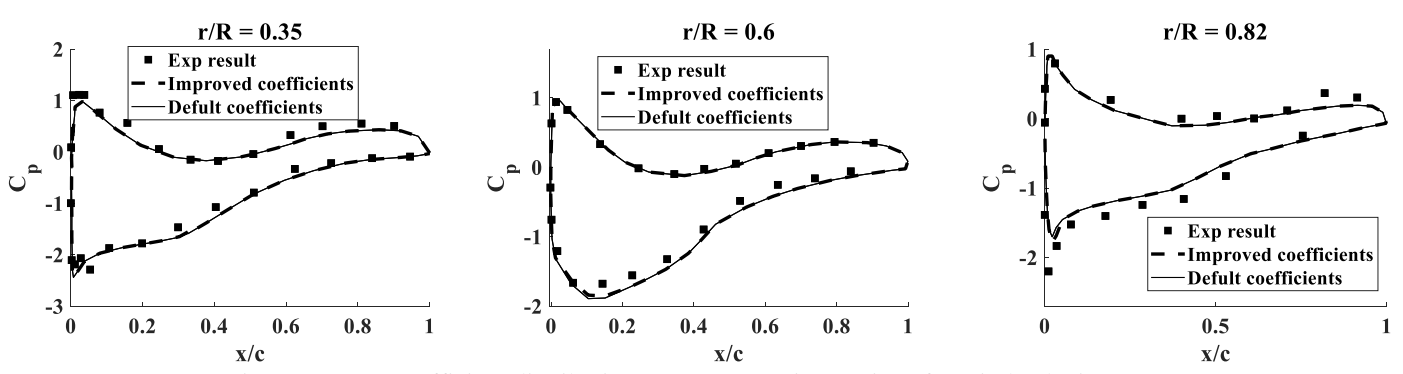


Fig 8. Pressure coefficient distributions at tree spanwise sections for wind velocity = 15 m/s

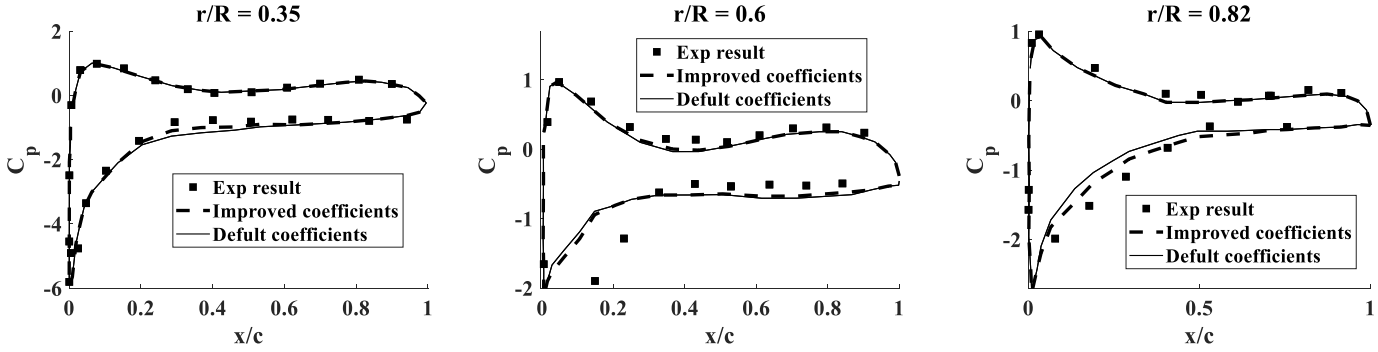


Fig 9. Pressure coefficient distributions at tree spanwise sections for wind velocity = 24 m/s

6. Conclusion

The improved accuracy of numerical simulations compared to experimental methods has significantly reduced both cost and time, while also enabling the integration of more optimized models into modern technologies. The standard k- ω SST turbulence model typically relies on default coefficients, which often lead to repetitive results. In this study, these coefficients were modified and replaced with improved sets to evaluate their effect on the aerodynamic performance of the three-dimensional Mexico rotor at three wind speeds. The results showed that each set offered varying improvements depending on the flow conditions: the first set performed better at 10 m/s, while the second set yielded superior results at 15 and 24 m/s. These findings suggest that the enhanced k- ω SST model provides more accurate predictions than the classical approach.

References

- [1] B. Plaza, R. Bardera, and S. Visiedo, "Comparison of BEM and CFD results for MEXICO rotor aerodynamics," Journal of Wind Engineering and Industrial Aerodynamics, vol. 145, pp. 115–122, 2015.
- [2] Darbandi, M., Jalali, R. and Schneider, G. E., "Megawatt wind turbine far wake and performance predictions using the unsteady actuator line model," 34th Wind Energy Symposium, San Diego, California, USA, 4-8 January 2016, pp. 1519
- [3] A. Bouhelal, A. Smaili, O. Guerri, and C. Masson, "Numerical investigation of turbulent flow around a recent horizontal axis wind turbine using low and high Reynolds models," Journal of Applied Fluid Mechanics, vol. 11, no. 1, pp. 151–164, 2018, published by Isfahan University of Technology.
- [4] P. G. Regodeseves and C. S. Morros, "Unsteady numerical investigation of the full geometry of a horizontal axis wind turbine: Flow through the rotor and wake," Energy, vol. 202, p. 117674, 2020, published by Elsevier.
- [5] D. Garcia-Ribeiro, V. Malatesta, R. C. Moura, and H. D. Cerón-Muñoz, "Assessment of RANS-type turbulence models for CFD simulations of horizontal axis wind turbines at moderate Reynolds numbers," Journal of the Brazilian Society of Mechanical Sciences and Engineering, vol. 45, no. 11, p. 566, 2023.
- [6] Darbandi, M., Schneider, G. E., Tahani, M., & Nojavan, A. (2025). Improving the k-ω SST Turbulence Model to Perform the Numerical Calculation for the Darrieus Vertical-Axis Wind Turbine Profiles. Proceedings of the AIAA SCITECH 2025 Forum, pp. 0028.
- [7] F. R. Menter, "Two-equation eddy-viscosity turbulence models for engineering applications," AIAA Journal, vol. 32, no. 8, pp. 1598–1605, 1994.
- [8] C. L. Rumsey, "Consistency, verification, and validation of turbulence models for Reynolds-averaged Navier–Stokes applications," Proceedings of the Institution of Mechanical Engineers, Part G: Journal of Aerospace Engineering, vol. 224, no. 11, pp. 1211–1218, 2010.
- [9] D. Garcia-Ribeiro, J. A. Flores-Mezarina, P. D. Bravo-Mosquera, and H. D. Cerón-Muñoz, "Parametric CFD analysis of the taper ratio effects of a winglet on the performance of a horizontal axis wind turbine," Sustainable Energy Technologies and Assessments, vol. 47, p. 101489, 2021.